

Agglomerate and ignition characteristics of aluminum particles in AN composite propellants

Kenichi Takahashi^{*†}, Keita Nakadai^{*}, Sho Oide^{*}, Mitsuaki Tanabe^{*},
Takuo Kuwahara^{*}, and Toru Shimada^{**}

^{*}Department of Aerospace Engineering, College of Science & Technology, Nihon University
7-24-1 Narashinodai, Funabashi, Chiba 274-8501, JAPAN
Phone: +81-47-469-5402

[†]Corresponding address: takahasi@aero.cst.nihon-u.ac.jp

^{**}Institute of Space and Astronautical Science, Japan Aerospace Exploration Agency
3-1-1 Yoshinodai, Chuo, Sagamihara, Kanagawa 252-5210, JAPAN

Received: December 6, 2011 Accepted: April 19, 2013

Abstract

Ammonium nitrate (AN) composite propellants are environmentally friendly, chlorine-free propellants. To improve the burning rate of composite propellant, aluminum particles are added as an extra energy ingredient for many composite propellants. However, the effects of agglomerate and ignition of aluminum particles on the temperature profile in the reaction zone near the burning surface and on the burning rate have not been studied well for aluminized AN composite propellants. The temperature profile in the reaction zone affects the burning rate. Therefore, it is important to investigate the effects of agglomerate and ignition of aluminum particles on the temperature profile. This study specifically addressed the effects of agglomerate and ignition of aluminum particles on the temperature profile in the reaction zone of aluminized AN composite propellant. Aluminum particles agglomerated on the burning surface. Then they were ignited near the burning surface. When agglomerates of aluminum particles ignited and burned near the burning surface, the temperature profile in the reaction zone was affected, which changed the burning rate.

Keywords : agglomerate, aluminum, ammonium nitrate, ignition, temperature profile

1. Introduction

Ammonium perchlorate (AP) has been used as an oxidizer in AP composite propellants for solid rockets. Hydrogen chloride (HCl) emissions from AP composite propellant are an important concern because of their demonstrated impact on the environment. Ammonium nitrate (AN) composite propellants are environmentally friendly and chlorine-free propellants¹⁻³. As an alternative oxidizer without chlorine (Cl) to AP, AN use has been attempted, but its higher hygroscopicity and lower burning rate than those of other oxidizers render it difficult to use practically. To improve these shortcomings, adding aluminum, modified AN such as PSAN, and adding AP as another oxidizer have been studied^{2,6}; various other challenges have been investigated.

Aluminized AN composite propellants present shortcomings related to aluminum which are similar to

those of aluminized AP composite propellants. This problem is agglomeration of aluminum particles on the burning surface. Agglomeration of aluminum particles has been studied by many researchers for many years⁷⁻⁹. Particularly, agglomeration of aluminum particles has been investigated experimentally and theoretically in aluminized AP composite propellants⁸⁻¹⁴. Agglomeration and ignition of aluminum particles in aluminized AN composite propellants differ from those in aluminized AP composite propellants. In aluminized AP composite propellants, aluminum particles aggregate and agglomerate on the burning surface to a diameter of about 300 μm , at which temperature they ignite immediately near the burning surface^{7-9,14}. However, in aluminized AN composite propellants, the agglomerate diameter is about 1000 μm . Therefore, ignition is delayed¹⁵.

The effects of agglomerate and ignition of aluminum

particles on temperature profile in the reaction zone of aluminized AN composite propellants has not been well studied. Because the temperature profile in the reaction zone of composite propellants affects the burning rate¹⁶⁾, it is important to investigate the effects of agglomerate and ignition of aluminum particles on the temperature profile.

This study specifically addressed the effects of the agglomerate and ignition of aluminum particles on the temperature profile in the reaction zone near the burning surface of aluminized AN composite propellant. The agglomerate diameter and ignition of aluminum particles near the burning surface were observed with a high-speed video camera and temperature profiles in the reaction zone were measured using a fine thermocouple. In addition, agglomerated aluminum particles were collected in the luminous flame and on the burning surface. We measured their diameters and observed those shapes. The effects of ignited aluminum particles as a heat source on the temperature profile in the reaction zone were investigated using CFD simulation.

2. Experiments

2.1 Solid propellant samples

Aluminized AN composite propellant samples were made with the compositions shown in Table 1. Ethyl carbamate was selected as a binder and activated carbon as a catalyst for ignition at low pressure and to maintain spontaneous combustion. To compare the effects of aluminum particles on the temperature profile in the reaction zone near the burning surface, samples were prepared with and without Al-added. The samples were molded with constant pressure compression. Having about 10 mm in diameter and 10 mm in height, they were formed into a cylindrical shape, as presented in Figure 1. To perform end burning, the exterior of the samples was coated with a vinyl-based adhesive^{17,18)}.

To measure the temperature profiles in the reaction zone near the burning surface, fine thermocouple (Pt-Pt 10%Rh, 12.5 μm wire diameter) was embedded in the center of the sample. Temperature profiles in the reaction zone near the burning surface were measured with the regression of the burning surface^{17,18)}.

When the thermocouple was embedded, we used "Yamatonori" (water-based glue) as an adhesive. Based on a comparison of Yamatonori with a superglue, an epoxy-based adhesive, and a vinyl-based adhesive, we chose Yamatonori because we were able to glue with it best. While adhering, we vaporized water because we applied the adhesive thinly to avoid too much infiltration into a sample and adhered it. The water-based adhesive did not affect our experiment results.

Figures 2 and 3 show an end face of the sample and a magnified image of the bonding plane. The magnified image of Figure 3 is equivalent to the "Magnified area" in Figure 2. The bonding plane adheres tightly as shown in Figure 3, in the thickness of the void, which is near to thermocouple wire diameter. Alternatively, the adhesive is not visible, it is adhered sufficiently homogeneously without a gap.

Table 1 Composition of samples.

		Al non-added [parts]	Al-added [parts]	Average diameter [μm]
Oxidizer	Ammonium nitrate (AN)	85	85	100
Binder	Ethyl carbamate (EC)	15	15	
Catalyst	Activated carbon (AC)	7	7	15
Metal fuel	Aluminum particle (Al)	0	10	7

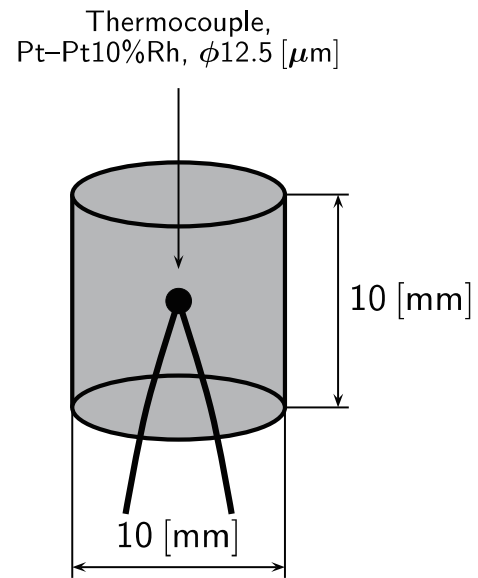


Figure 1 Solid propellant sample.

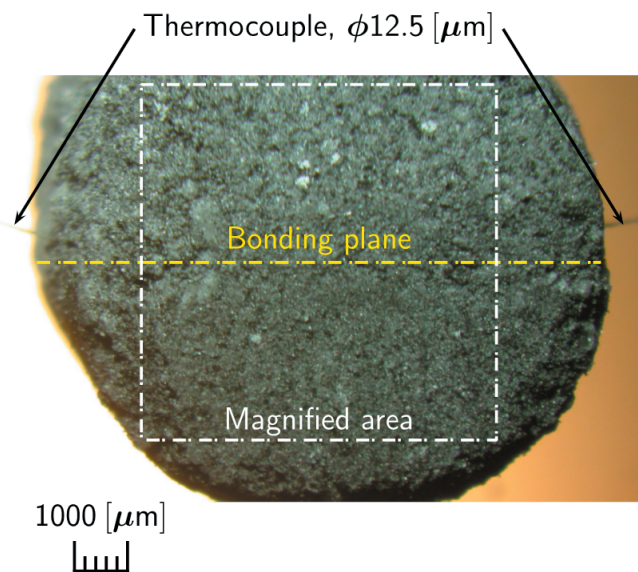


Figure 2 End face of the sample.

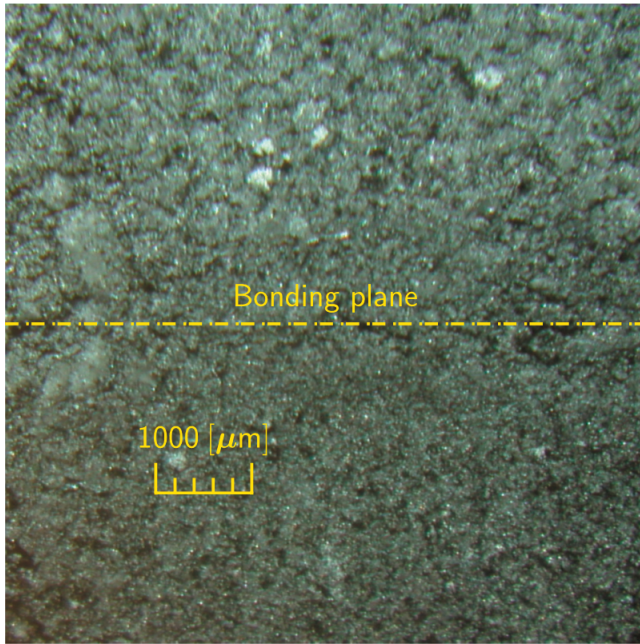


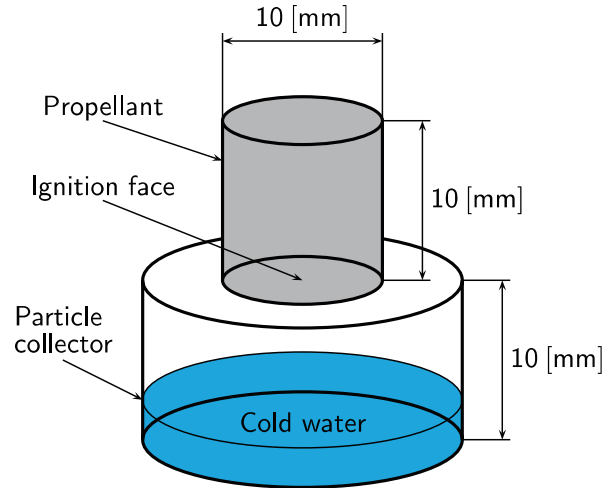
Figure 3 Magnified image of the bonding plane.

2.2 Strand burner

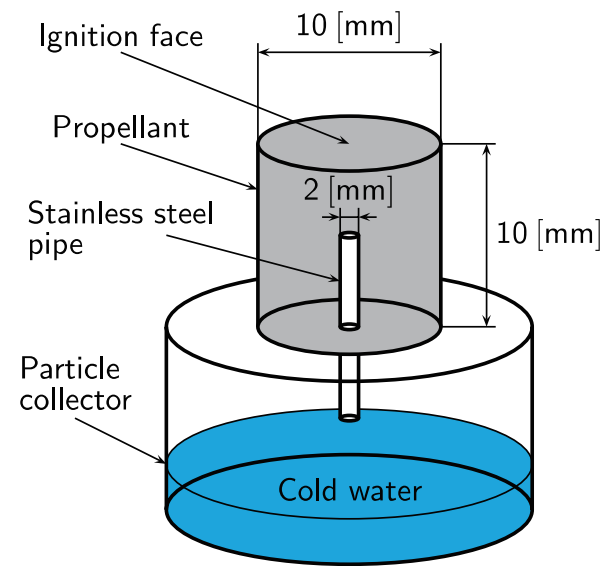
The solid propellant samples were burned in the strand burner as presented in Figure 4. Experimental conditions were a nitrogen atmosphere, 1.5 MPa initial pressure, and 293K (20°C) initial temperature. The experiments were repeated 10 times for each sample.

2.3 Particle collector

Figure 5 presents the solid propellant samples with particle collectors in the luminous flame and on the burning surface. They were set in the strand burner. While the sample is combusting, the aluminum particles in the luminous flame are caught in the cold water, as shown in Figure 5(a). We embedded the stainless steel pipe (2 mm inner diameter) in the center of the sample as shown in Figure 5(b). While the sample is combusting, the pipe appears on the burning surface. The aluminum particles on the burning surface are sucked into the pipe and fall into the cold water by a pressure difference between the burning surface and the ambient gas. The collected



(a) Collector in the luminous flame.



(b) Collector on the burning surface.

Figure 5 Particle collectors.

aluminum particles dried naturally. Then we measured the aluminum particle diameters from SEM images and observed the particle shapes.

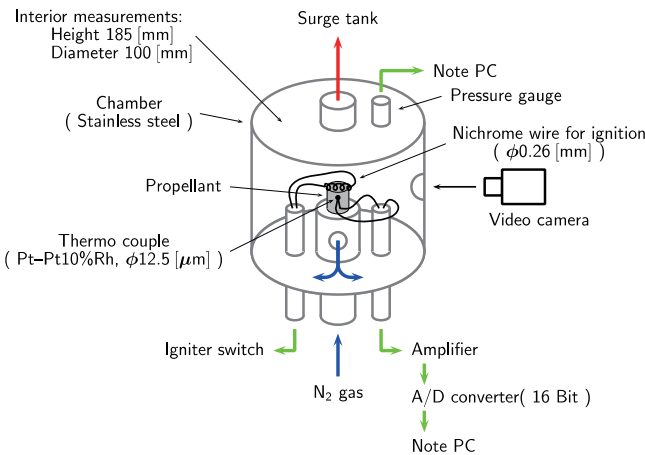


Figure 4 Strand burner.

3. Numerical analysis with CFD simulation

OpenFOAM (Open source CFD toolbox; OpenCFD Ltd., UK) was used for CFD simulation. The simulation was conducted using three-dimensional finite volume method. The solver was “reacting Foam” included in OpenFOAM. In this study, chemical reactions and turbulence models included this solver were not used. SALOME (Open source software for pre-processing and post-processing; Open CASCADE, France) was used for domain and mesh generation. The mesh was a non-structured mesh by tetrahedra. The simulation was performed in a cylindrical domain.

The ignited aluminum particles were assumed as a spherical heat source. The temperature distribution by the heat transfer from the particle as a heat source was

Table 2 Conditions of CFD simulation.

Initial and inlet conditions	Laminar flow
	Velocity : 2 [m s ⁻¹]
	Temperature : 500 [K]
Particle	Spherical particle
	Particle diameter : 160 [μm]
	Surface temperature : 3000 [K]

examined specifically. Heat transfer was accomplished by the working fluid. The particle diameter was the average diameter from experimentally obtained results from Figure 10 in Section 4.2. The particle surface temperature was referred from another report⁹.

The initial and inlet conditions were obtained from results of experiments and theoretical calculations. Nitrogen gas was used as the working fluid.

The conditions of the simulation are presented in Table 2.

4. Results and discussion

4.1 Burning rate

The burning rate was calculated from the length of the sample and the combustion time, which were measured using a high-speed video camera. The burning rates are depicted in Figure 6.

By adding aluminum particles, the burning rate increased and the pressure sensibility decreased. These results resemble those of previous studies³. The burning rate changed by ignition and burning of aluminum particles, indicating that added aluminum particles are effective at improving the burning rate.

In this experiment, the effect of adding aluminum particles was confirmed. However, details of the effects of aluminum particles are unknown. Enhancement of the burning rate is regarded as related with the effects of aluminum particles on the temperature profile in the

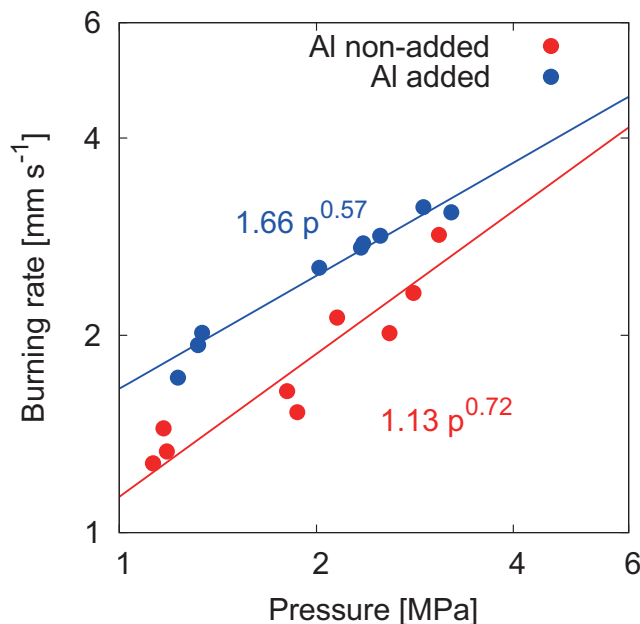


Figure 6 Burning rate.

reaction zone. Where aluminum particles ignite and the diameter of agglomerated aluminum particles are investigated in later sections.

4.2 Agglomeration of aluminum particles

Agglomeration of aluminum particles on the burning surface was observed using a high-speed video camera, as portrayed in Figure 7.

Aluminum particles aggregate on the burning surface. They agglomerate in a spherical shape. Then they begin oxidation or ignition, and detach from the burning surface. This behavior resembles that reported for aluminized AP composite propellant^{8,9} and other studies^{2,15}. However, aggregates of irregular shapes are also present on the burning surface, with diameter of 1000 μm or greater. These are much larger than the diameter of about 300 μm found for aluminized AP composite propellant.

Figure 8 presents SEM images of the aluminum particles collected on the burning surface. The aluminum particles are aggregated and melted as shown in Figure 8 (a). Because the aggregated aluminum particles are round, they melt. Furthermore, it becomes the particle in Figure 8(b) when the particle in Figure 8(a) continues to aggregate and melt. It is considered that "Aggregated and melting aluminum" in Figure 7 is similar to Figure 8(b).

Agglomerate diameters of aluminum particles on the burning surface were measured from high-speed video camera images as presented in Figures 9 and 10. Regression distance of the burning surface was calculated with the time of agglomeration on the burning surface and the burning rate. The particles in the high-speed video camera images have a blurred outline. The inside almost becomes the white by the luminous flame. When we measure the diameters of the particles from the images, we measure the diameter of the part of the white area inside the blurred outline (luminous flame zone).

In Figure 9, the regression distance from about 1 μm to 90 μm is shorter than the reaction zone, which has

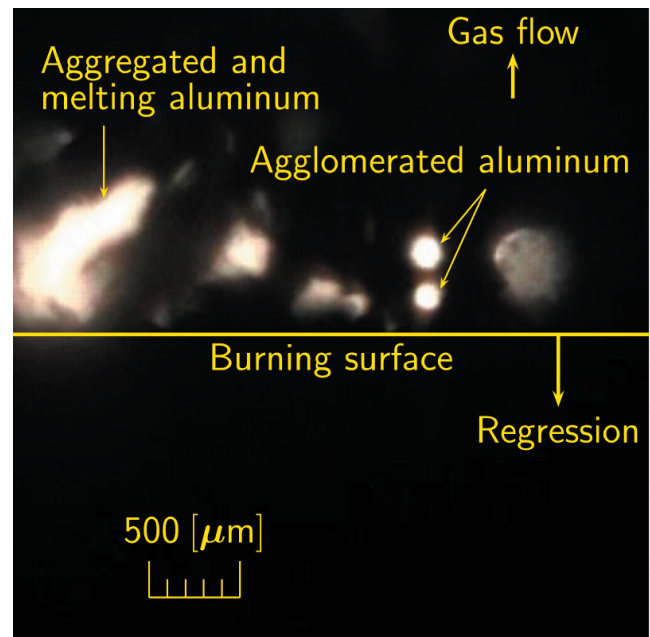
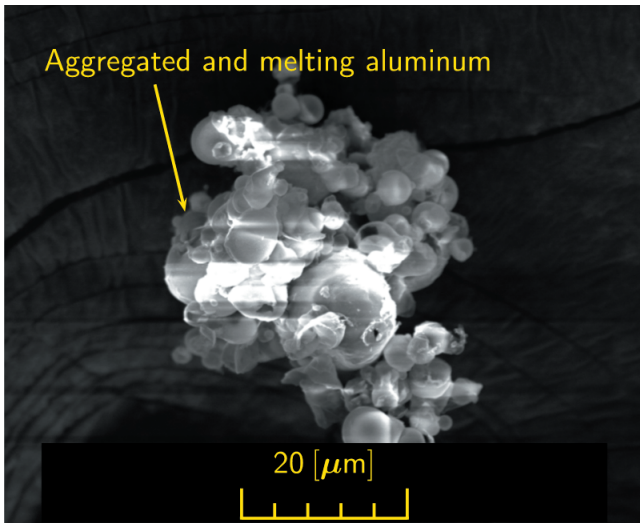
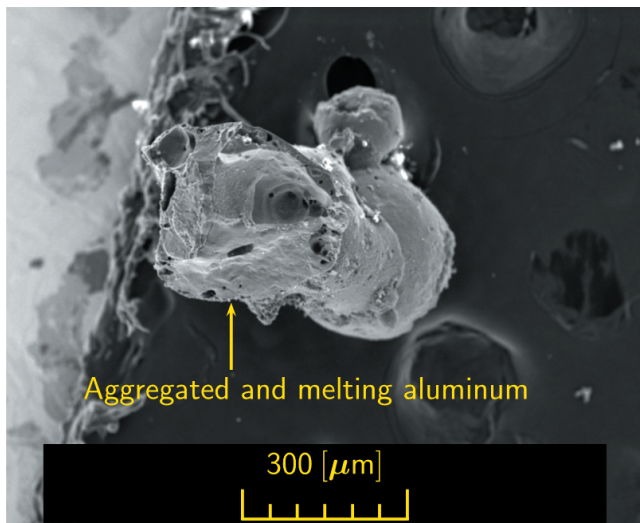


Figure 7 Aluminum particles near the burning surface.



(a)



(b)

Figure 8 SEM images of aggregated and melting aluminum particles on the burning surface.

thickness of about $700\mu\text{m}$, as described in Section 4.4. Agglomerate diameters of aluminum particles are distributed from about $30\mu\text{m}$ to $400\mu\text{m}$, with average diameter of $160\mu\text{m}$, as depicted in Figure 10. These diameters do not include irregular shapes because they were unable to ignite near the burning surface. In the regression of the burning surface from about $1\mu\text{m}$ to $90\mu\text{m}$, aluminum particle agglomerates from about $30\mu\text{m}$ to $400\mu\text{m}$ appeared.

Figure 11 shows the agglomerate diameter distribution in the luminous flame. In Figures 10 and 11, there is a peak at about $160\mu\text{m}$. The distributed range almost agrees. When the aluminum particle combusts, the diameter decreases. However, because the burning time from the reaction zone to the luminous flame is short, the change of the diameter is small. Therefore the diameter distribution of the luminous flame is similar to that of the reaction zone, and the accuracy of the diameter distribution in the reaction zone is confirmed.

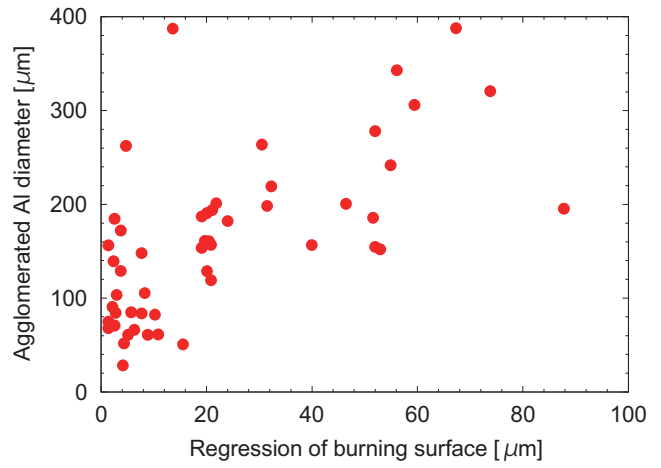


Figure 9 Agglomerate diameter in the reaction zone.

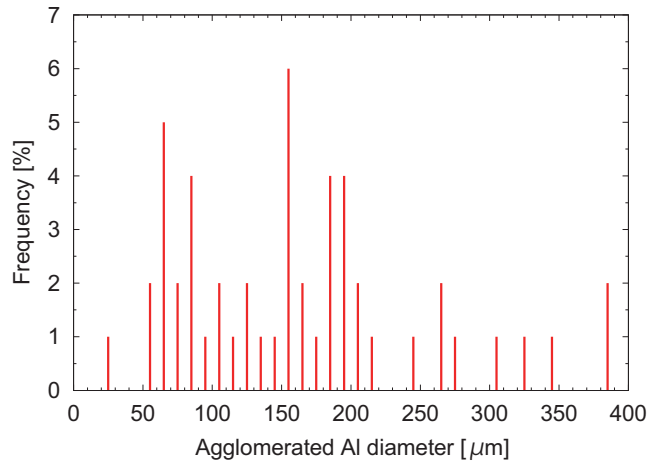


Figure 10 Agglomerate diameter distribution in the reaction zone.

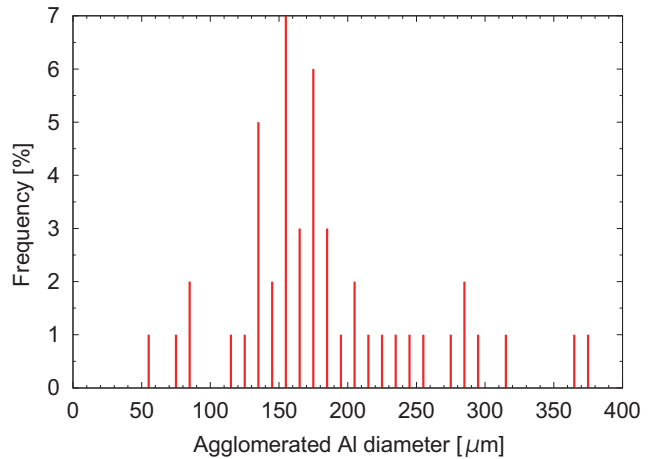
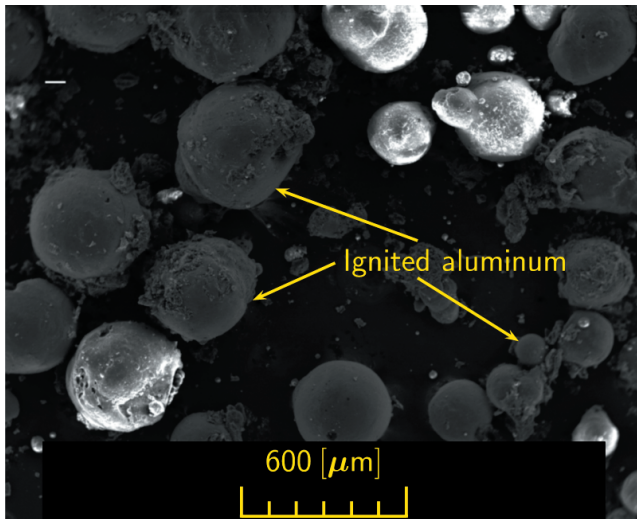


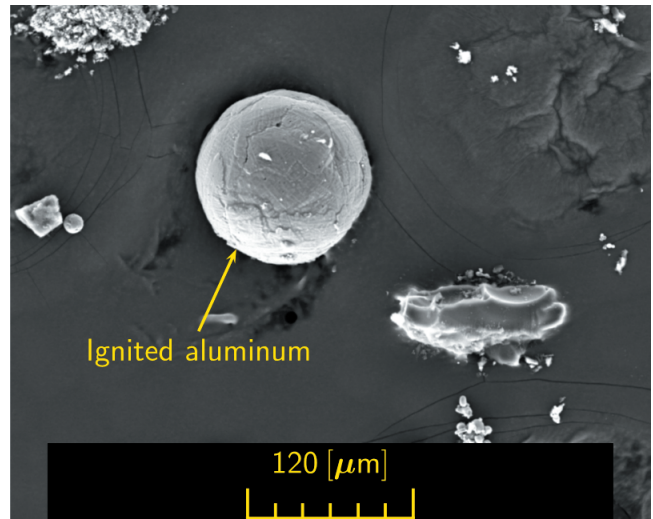
Figure 11 Agglomerate diameter distribution in the luminous flame.

4.3 Confirm agglomeration and ignition of aluminum particles

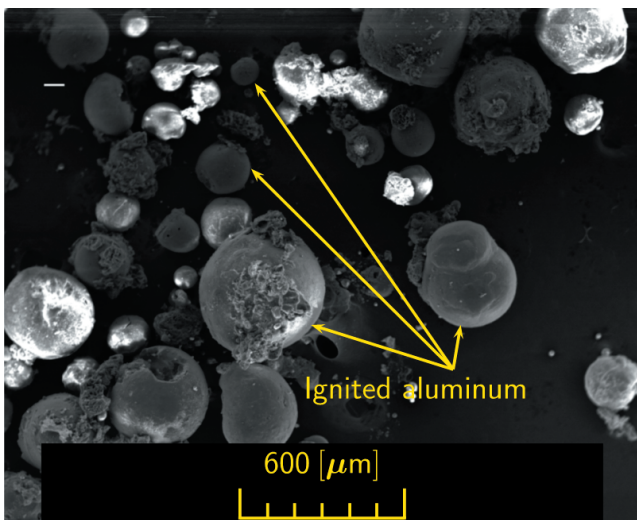
Figures 12 and 13 present SEM images of the aluminum particles which were collected in the luminous flame and on the burning surface. In figures, the ignited aluminum particles are denoted as “Ignited aluminum”. We show the different particles of representative particle diameters. They agglomerated, became spherical, and ignited as shown in Figure 12. They were combusting when they



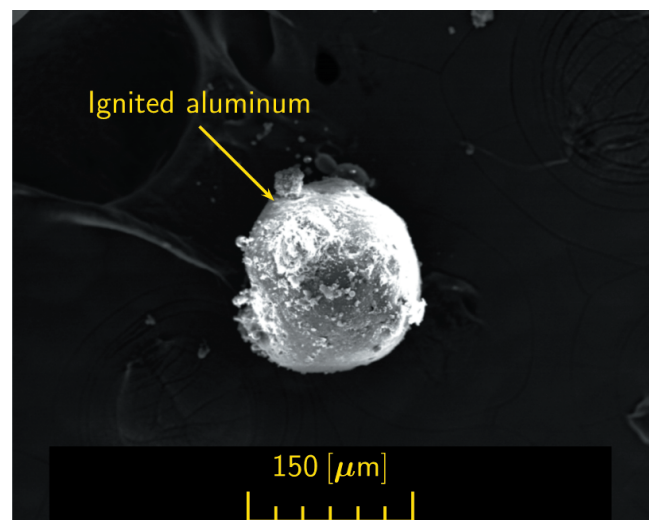
(a)



(a)



(b)



(b)

Figure 12 SEM images of aluminum particles in the luminous flame.

Figure 13 SEM images of aluminum particles on the burning surface.

were collected. The aluminum particles in Figure 13 are similar to those in Figure 12. Therefore the particles in Figure 13 were ignited. Ignited aluminum particles were present near the burning surface. Furthermore, because the aluminum particles are spherical in Figures 12 and 13, agglomeration of the aluminum particles was confirmed.

We defined a particle that is agglomerated in a spherical shape and which becomes white by luminous flame as an ignited aluminum particle. We show the ignited aluminum particle as "Agglomerated aluminum" in Figure 7.

4.4 Influence of voids in the solid propellant sample on the temperature profile

The voids are in the solid propellant sample, because the sample is composed of the crystalline oxidizer with the binder, the catalyst, and the metal fuel, and it is compaction-molded at constant pressure. The void ratio becomes 9% without Al addition, 7% by the Al 10% added. The combustion gas decreases at a void, and a temperature fluctuation is caused, however, it is considered that its fluctuation differs from the fluctuation

by an ignited and burning aluminum particle. The phenomenon by which temperature falls greatly near the burning surface in the temperature profile irrespective of aluminum particles addition or not was not observed, it is considered that the influence of the voids is small in the experiment used for this study, and we take no thought of the influence in next section.

4.5 Temperature profile near the burning surface

Temperature profiles near the burning surface are shown in Figures 14 and 15. Because the width of the temperature fluctuation of Figure 15(a) is $400\mu\text{m}$, the movement speed of the aluminum particle by the observation of a high-speed video camera is 0.2m s^{-1} . Therefore the time passage near the thermocouple is 2 ms. When the ambient temperature is 1200 K, the time constant of the thermocouple in this study is 0.015 ms. Therefore, the response of the thermocouple is sufficient for this study.

The temperature profile of Al non-added sample is portrayed in Figure 14. The burning surface is located at 0

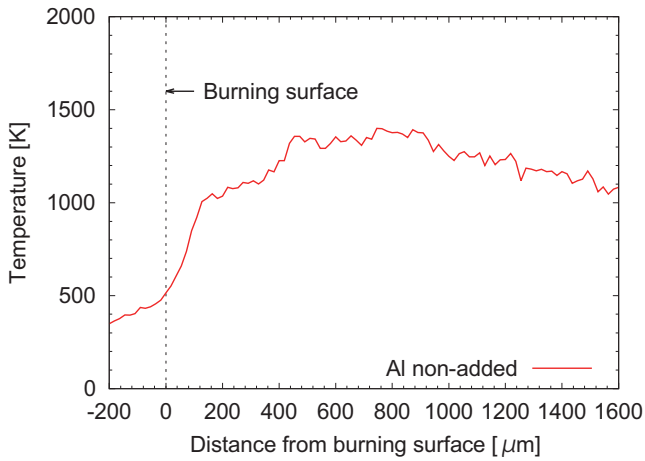


Figure 14 Temperature profile of the Al non-added sample.

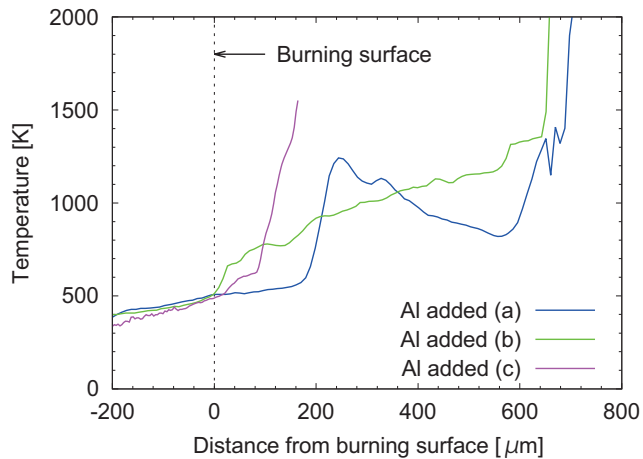


Figure 15 Temperature profile of Al-added sample.

μm . The burning surface was determined at the location with a changing temperature gradient from solid phase to gas phase^{7),19),20)}. In the reaction zone, temperatures rise rapidly to about $200\mu\text{m}$, as portrayed in Figure 14. The temperature rises slowly to about $500\mu\text{m}$ near the flame zone. The reaction zone thickness is about $500\mu\text{m}$.

For the Al-added sample, the reaction zone thickness is about $700\mu\text{m}$, because temperature rises rapidly at about $700\mu\text{m}$ near the flame zone as presented in Figures 15(a) and 15(b). Temperature fluctuation occurs at about $250\mu\text{m}$, and the temperature fluctuation reaches about $400\mu\text{m}$ width. The temperature fluctuation in Figure 15(a) was not observed in the Al non-added sample in Figure 14, because of the temperature fluctuation caused by ignited aluminum particle, which ignited up to the regression distance of about $250\mu\text{m}$. Rapid temperature rising at about $200\mu\text{m}$ is caused by the ignited aluminum particle, the rapid rising is similar to the rising at about $100\mu\text{m}$ as shown in Figure 15(c). The temperature profile of Figure 15(c) is cut off by the ignited aluminum particle at about $160\mu\text{m}$, the rapid temperature rising is occurred near the ignited particle. Aluminum particles produce a diffusion flame by burning in the gas phase, reaching a temperature of about $3000\text{--}4000\text{K}$ ⁹⁾. Then the particle produces a higher temperature area than that around the gas temperature. Details related to the temperature distribution around the particle are described in the next section. The reason why

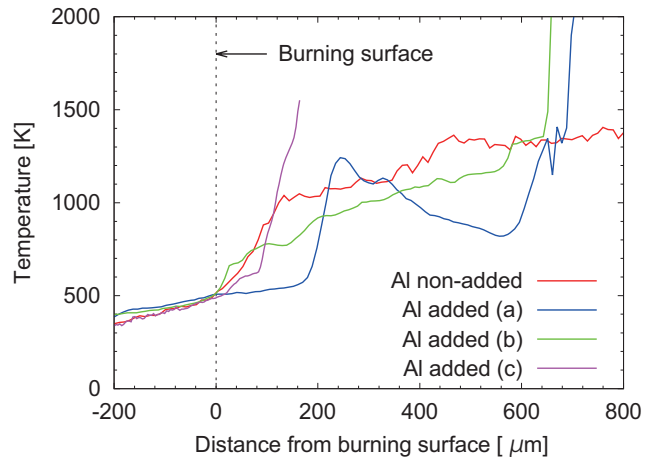


Figure 16 Temperature profiles of Al non-added and added samples.

the peak temperature of this temperature fluctuation as in Figure 15(a) is lower than $3000\text{--}4000\text{K}$ is that the ignited aluminum particle is distant from the thermocouple.

Because the aluminum particles aggregate on the burning surface, some diameters in them are about $1000\mu\text{m}$, they affect reaction mechanism in the reaction zone near the burning surface. Therefore the temperature profile in the reaction zone is affected, and the low temperature profile occurs as shown in Figure 15(a) from $0\mu\text{m}$ to $160\mu\text{m}$.

The agglomerated aluminum particle diameter and the appearance are irregular. The small influence of the agglomerated aluminum particle in the temperature profile might occur. In such cases, the temperature profile is similar to that of Figure 15(b).

When the burning aluminum particle is close to the thermocouple, the temperature fluctuation is measured. The location and the width of the temperature fluctuation are regarded as related to the diameter, the amount, and the agglomeration of aluminum particles.

Figure 16 presents a comparison of temperature profiles with aluminum particles non-added or added. Figure 16(c) is cut off by the ignited aluminum particle. The cutting position is in the reaction zone near the burning surface. The temperature soars immediately before cutting. The temperature around the ignited aluminum particle is higher than that with no addition of Al. The temperature fluctuations caused by ignited aluminum particles as in Figure 16(a) or 16(c) are distributed in the reaction zone. The temperature rises by the ignited aluminum particle in this way, the temperature in the reaction zone near the burning surface rises on average, and the temperature gradient near the burning surface increases. When the aluminum particle ignites near the burning surface, the temperature in the reaction zone is affected and altered, and the burning rate is affected. However, the heterogeneous combustion wave is stronger in the aluminized sample, as shown in Figures 16(a) and 16(c).

4.6 Ignited aluminum particles as a heat source

The temperature distribution around an aluminum

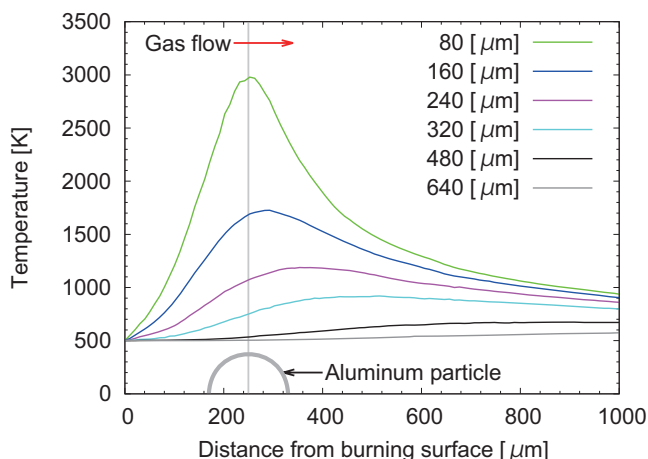


Figure 17 Temperature distribution near the heat source.

particle in aluminized AP composite propellant was examined in our previous study¹⁷. The CFD simulation was performed using the same CFD tool as that used in this study to evaluate the effects of the temperature distribution around an ignited aluminum particle as a heat source.

In this section, the relation between the temperature fluctuation in the temperature profile and the temperature distribution around the ignited aluminum particle was investigated using the CFD simulation.

When the ignited aluminum particle of the diameter of 160 μm becomes a heat source, the temperature distribution near the particle as a heat source is like that presented in Figure 17, which shows temperature profiles as lines along the gas flow direction (indicated in the figure). The forms of the temperature profile and the peak temperature are shown according to the distance from the particle. These lines are 80–640 μm distant from the center of the particle. The particle is put at 250 μm distance from the burning surface. The temperature around the particle is higher than the gas temperature of 500 K. It is about 1000–3000 K. Close to the particle, the temperature increases; moreover, the temperature profile becomes sharper.

The temperature fluctuation at around 250 μm in the temperature profile of Figure 15(a) becomes the fluctuation width of 400 μm and the peak temperature of 1200 K, which almost agrees with the temperature profile of around 160 μm (blue line) to 240 μm (magenta line) away from the particle. The peak temperature differs according to the distance from the particle. The fluctuation width changes according to the particle diameter. In this way, we are able to estimate the distance from the particle and the particle diameter by the temperature fluctuation in the temperature profile. We are able to estimate the temperature fluctuation of Figure 15(a) by the ignited aluminum particle, which has approx. 160 μm diameter and which is around 160 μm to 240 μm distant from the thermocouple. In addition, when the thermocouple is cut off, it is similar to a temperature profile from around 80 μm (green line) to 160 μm (blue line), the tendency that the temperature soars almost accords with Figure 15(c) because the ignited aluminum particle came extremely

close to the thermocouple.

5. Conclusion

After addition of aluminum particles to AN composite propellant, the burning rate increased and the pressure sensibility decreased. The process of aggregation and agglomeration of aluminum particles on the burning surface was observed. These are similar to results obtained in earlier studies^{2), 3), 15)}.

In the aluminized AN composite propellant examined in this study, aluminum particles aggregate and agglomerate on the burning surface. Then some of them ignite in the reaction zone near the burning surface. When agglomerates of aluminum particles ignite and burn near the burning surface, the temperature profile in the reaction zone is affected, thereby changing the burning rate.

Acknowledgement

This work was sponsored by the Foundation for the Promotion of Industrial Explosives Technology 2009–2011.

References

- 1) C. Oommen and S. R. Jain, *Journal of Hazardous Materials*, A67, pp. 253–281, (1999).
- 2) V. Babuk, A. Glebov, I. Dolotkazin, A. Dosychev, L. T. De Luca, B. D'Andrea, A. Vorozhtsov, and G. Klyakin, *European Conference for Aero-Space Sciences*, (2005).
- 3) V. P. Sinditskii, V. Y. Egorshv, D. Tomasi, and L. T. De Luca, *Journal of Propulsion and Power*, 24, 1068–1078, (2008).
- 4) T. Kuwahara and N. Shinozaki, *Kogyo Kayaku (Science and Technology of Energetic Materials)*, 53, 131–136, (1992).
- 5) S. Yoshida and M. Kohga, *Science and Technology of Energetic Materials*, 67, 117–123 (2006).
- 6) S. Levi, D. Signoriello, A. Gabardi, M. Molinari, L. Galfetti, L. T. De Luca, S. Cianfanelli, and G. F. Klyakin, *Progress in Propulsion Physics*, 1, 97–108, (2009).
- 7) N. Kubota, "Propellant Handbook", Propellant Committee, Japan Explosives Society, (2005).
- 8) K. Kuo and M. Summerfield, *Progress in Astronautics and Aeronautics*, 90, 1–47, 479–505, (1984).
- 9) V. Yang, T. B. Brill, and W.-Z. Ren, *Progress in Astronautics and Aeronautics*, 185, 267–283, 287–332, 663–684, 689–719, 723–744, (2000).
- 10) V. A. Babuk, V. A. Vasilyev, and M. S. Malakhov, *Journal of Propulsion and Power*, 15, 783–793, (1999).
- 11) O. G. Glotov, *Combustion, Explosion, and Shock Waves*, 36, 476–487, (2000).
- 12) H. Habu, "Study on Hydrogen Chloride Suppression in Exhaust gas of Composite Propellant by Magnalium", Ph. D. Thesis, University of Tokyo, (2002).
- 13) H. Habu, T. Shimada, and H. Hasegawa, 42nd AIAA/ASME/SAE/ASEE Joint Propulsion Conference, AIAA Paper 2006–5249, (2006).
- 14) F. Maggi, A. Bandera, and L. T. De Luca, 46th AIAA/ASME/SAE/ASEE Joint Propulsion Conference, AIAA Paper 2010–6751, (2010).
- 15) L. T. De Luca, C. Paravan, A. Reina, E. Marchesi, F. Maggi, A. Bandera, and G. Colombo, 46th AIAA/ASME/SAE/ASEE Joint Propulsion Conference, AIAA Paper 2010–

- 6752, (2010).
- 16) N. Kubota, WILEY-VCH Verlag GmbH & Co. KGaA, (2007).
- 17) K. Takahashi, T. Mano, M. Tanabe, T. Kuwahara, and T. Shimada, 46th AIAA/ASME/SAE/ASEE Joint Propulsion Conference, AIAA paper 2010, 6679, (2010).
- 18) K. Nakadai, K. Takahashi, M. Tanabe, and T. Kuwahara, 47th AIAA/ASME/SAE/ASEE Joint Propulsion Conference, AIAA Paper 2011, 5713, (2011).
- 19) A. J. Sabadell, J. Wenograd, and M. Summerfield, AIAA Journal, 3, 1580–15584, (1965).
- 20) N. Kubota, T. Kuwahara, and S. Miyazaki, 20th AIAA/ASME/SAE/ASEE Joint Propulsion Conference, AIAA Paper 1984, 1435, (1984).

AN系コンポジット推進薬でのアルミニウム粒子の集塊と着火の特性

高橋賢一^{*†}, 中臺啓太^{*}, 生出翔^{*}, 田辺光昭^{*}, 桑原卓雄^{*}, 嶋田徹^{**}

AN系コンポジット推進薬は非塩素で低負荷環境の固体推進薬である。AN系コンポジット推進薬は燃焼速度が遅いことが問題となっており、アルミニウム粒子を添加することにより改善できる。燃焼速度を改善するための金属燃料としてのアルミニウム粒子は様々な固体推進薬に添加されている。燃焼表面近傍の反応層内の温度分布と燃焼速度へのAN系コンポジット推進薬に添加されるアルミニウム粒子の集塊と着火の影響はよく解っていない。燃焼速度は燃焼表面近傍の反応層内の温度分布の影響を受けるので、アルミニウム粒子の集塊と着火が温度分布へ与える影響を詳細に調べることが重要となる。本研究では、アルミニウム粒子を添加したAN系コンポジット推進薬でのアルミニウム粒子の集塊と着火が燃焼表面近傍の反応層内の温度分布へ与える影響に注目した。アルミニウム粒子は燃焼表面上で集塊し、燃焼表面近傍の反応層内で着火した。集塊したアルミニウム粒子が燃焼表面近傍で着火し燃焼することで、反応層内の温度分布が影響を受け、燃焼速度が変化した。

* 日本大学理工学部航空宇宙工学科 〒274-8501 千葉県船橋市習志野台7-24-1
Phone: 047-469-5402

†Corresponding address: takahasi@aero.cst.nihon-u.ac.jp

** 宇宙航空研究開発機構宇宙科学研究所 〒252-5210 神奈川県相模原市中央区由野台3-1-1